Preparation of multifunctional polysaccharide microcontainers for lipophilic bioactive agents

*Tatiana N. Borodina * [a], Dmitry O. Grigoriev [b], Maria A. Carillo [b], Jürgen Hartmann [b], Helmuth Moehwald [b], Dmitry G. Shchukin [c]*

a Laboratory of Bioorganic Structures, Shubnikov Institute of Crystallography Russian Academy of Sciences, Moscow, Russia.

b Max Planck Institute of Colloids and Interfaces, Potsdam-Golm, Germany.

c Stephenson Institute for Renewable Energy, Department of Chemistry, The University of Liverpool, L69 4ZF Liverpool, United Kingdom.

KEYWORDS: microcontainer, hydrophobic bioactive agent, ultrasound, emulsification.

ABSTRACT: Chitosan/xanthan gum microcontainers with a core-shell structure formed due to chemical interactions between polysaccharide chains induced by ultrasonication are presented. Containers were prepared by sonication of water-immiscible (oil-like) liquids in the solution of polysaccharides. One-step fabrication of the container permanent shell is possible owing to contribution of ultrasonically caused formation of hydrogen bonds and amide linkages. We synthesized containers in a wide size range from 350 nm to 7500 nm varying an oil/water ratio. The microcontainers were modified with oppositely charged polyelectrolytes and microparticles which could be used to impart the specified properties to the system. The biocide 4,5-dichloro-2-

n-octyl-4- isothiazoline-3-one (DCOIT) was loaded into the proposed containers by utilizing its solution as an oil phase. The following incorporation of the DCOIT containers into polymer coating demonstrated more sustained antibacterial activity (around 30%) of the biocide in the encapsulated state compare to its non-encapsulated form.

INTRODUCTION

In spite of numerous methods successfully applied for fabrication of microscaled carriers filled by hydrophobic bioactive substances [1], continuous efforts are made to develop new encapsulation techniques because of necessity to obtain a stable delivery system by a simple and economic procedure. In most cases, water-immiscible components are encapsulated via emulsion route [2], which requires additional stabilization of a colloidal system by different types of surfactants, surface-active polymers, proteins, polysaccharides or their mixtures. Several techniques were developed up-to-date to produce emulsions, such as high pressure homogenization, microfluidization, membrane contractor technique, ultrasonication etc. [3-6]. The last technique is most promising for the simultaneous encapsulation of prepared emulsion droplets due to various sonochemical effects accompanying the ultrasonic comminution in a liquid/liquid system.

Ultrasound produces cavitations (the formation, growth and collapse of cavitation bubbles), which is an underlying primary cause of sonochemical effects [7]. The extreme conditions inside a cavitation bubble (5000K, 1000 atm) lead to various physical processes or/and chemical reactions creating spherical shells which contain either gas or liquid in their inner cavity. In the case of formation of microspheres under influence of ultrasound, the cavitation bubble played a role of a quasistable template with unique physico-chemical characteristics of the surface. The

mechanism responsible for microcapsule formation is a combination of two processes: emulsification and cavitation [1].

The microcapsules are fabricated in polymer solution layered over water-immiscible solvent by sonication in a shorter period than by the usual microencapsulation methods [8, 9]. A sonochemical encapsulation process has no demand on special equipment and materials: only sonotrode is required. The ultrasonic emulsification occurs in the mixture of polymer solution and water-immiscible liquid, which contains bioactive agents to be encapsulated. Microcapsule shells composed of polymer are synthesized at the interface between oil and the polymer solution within few minutes. Moreover, the one-step ultrasonically assisted encapsulation procedure is extremely effective in producing the microspheres with high encapsulation efficacy [10].

Suslick and co-workers were the first who demonstrate the successful application of high-intensity ultrasound to produce protein microspheres and fabricated by this sonochemical method microcontainers with shells made of proteins bovine serum albumin, human serum albumin, hemoglobin and myoglobin [11, 12]. The mechanism of protein shell formation was explained by effect on interaction of the free radicals generated during the sonication process on protein molecules leading to their cross-linking through disulfide bridges. Lately, Gedanken and co-workers synthesized protein microspheres from avidin and streptovidin, which do not possess sulfur-containing cysteine moieties [13]. In their opinion, hydrophobic interactions and thermal denaturation assist the sphere formation. Suslick et al. also obtained the polyglutamate spheres, which were stable in wide range of pH due to hydrogen bonding networks [14].

To date, several research groups followed this approach to fabricate various spheres/containers, utilizing different proteins or polymers with protein moieties, e.g. bovine serum albumin capsules were demonstrated in [15, 16], capsules from polyglutamic acid in [14,

17], α-amylase microspheres in [18], lysozyme microbubbles in [19], containers based on gum arabic in [20]. High biocompatibility and biodegradability of proteins as material for the containers' build-up can be considered as benefits for their potential application. On the other hand, relatively high costs of these substances as well as their low long-term stability significantly limit their universal use especially in the application fields other than biomedical one.

Here, we present a new class of oil filled microcontainers with core/shell morphology which can be prepared in one-step procedure applying a low-frequency ultrasound. The advantage of these microcapsules as compared to ones proposed earlier is the chemical nature of their shells made exclusively of polysaccharides, chitosan and xanthan gum, which stabilizes microcapsules in a broad pH range. The shell of the containers composed of two polymers which create a permanent structure of the system due to ultrasonically-induced chemical interactions between them. The previously demonstrated containers were mostly fabricated on the base of non-human protein types (such as bovine serum albumin), thus being quite allergenic. Therefore, the probability to get an immune response to proteins is much higher than to polysaccharides. On the other hand, human proteins are frequently very expensive [21, 22], making polysaccharides more attractive as shell components for the development of carriers for biomedical applications.

Chitosan possesses many useful biomedical properties including biocompatibility, biodegradability, bioactivity, fungistatic nature, lack of both toxicity and allergenicity [23]. Therefore, it is widely used in numerous applications ranging from pharmaceutical and cosmetic products to water treatment and plant protection [24]. Xanthan gum is also a fully biodegradable polymer stable over a broad pH range and exhibits several favorable rheological properties such

as high at-rest or low-shear viscosity and high pseudoplasticity [25]. It is widely used in various industry branches such as food, pharmaceutical or cosmetic industry [26].

RESULTS AND DISCUSSION

Chitosan and xanthan gum, as a polycation and polyanion respectively, can spontaneously form polyelectrolyte complex. Prevention of a complex formation is an important precondition for the ultrasonically assisted microcontainer fabrication applying these two polymers. To avoid electrostatic interaction between the polysaccharides in the mixture, pH values of their solutions were adjusted to the acidic. The dissociation of D-glucuronic acid and pyruvic acid units which determine [27] the character of Xanthan gum as a weak acid is in this pH range completely suppressed. On the contrary, primary amine groups of chitosan [28] are protonated in the same pH range providing its good solubility.

Figure 1 shows a scheme of microcontainer fabrication. The mixture of chitosan and xanthan gum was layered with non-aqueous liquid and exposed to high-intensity ultrasonication. Cross-linking of both polysaccharides due to chemical interactions between their amino, hydroxyl and carboxyl functional groups is induced by high energy ultrasound treatment. Production of highly reactive free radicals, such as $OH^{\cdot}$ and $H^{\cdot}$, during the acoustic cavitation in water [11] results in chemical reactions between functional groups located at the interface between a dispersed phase and a dispersion medium. It leads to the creation of a stable layer at the droplet surface and subsequently to the formation of permanent shells of microcontainers.

We applied the proposed method to fabricate the microcontainers loaded with different types of “oils” such as miglyol, soybean oil, hexane, cyclohexane and toluene. The change of oil phase had no effect on the colloidal stability of the system, which evidences that the chemical nature of

the oil used does not influence the generation of free radicals upon sonication and also does not participate in the shell formation process.

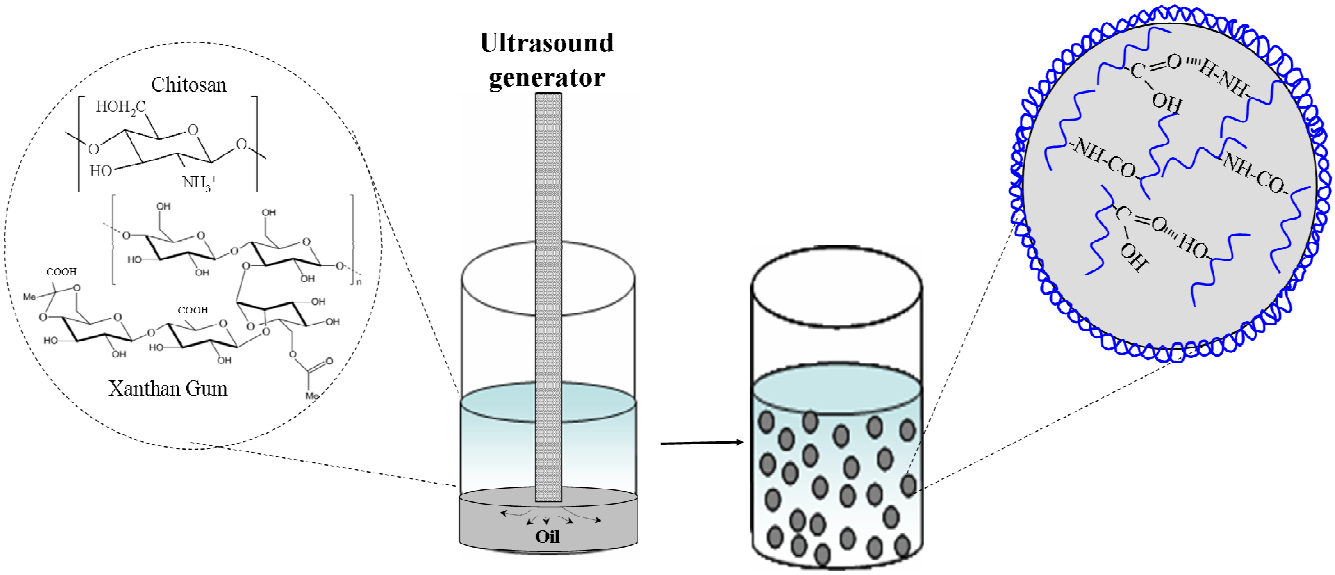

Figure 1. The schematic representation of the microcontainer formation.

We used FTIR spectroscopy to investigate chemical transformations induced by the sonication of the polymer mixture. Figure 2 shows spectra of chitosan, xanthan gum and their mixture extracted from the container shell in the range from 800 to 1800 cm^{-1} (full spectra are given in SI**)**. The band 1651 cm^{-1} (NH_2 deformation in primary amines) in the chitosan spectrum is shifted in the mixture spectrum to 1633 cm^{-1} (C=O stretch and NH_2 deformation in primary amides), while a peak at 1402 cm^{-1} in the xanthan gum spectrum (OH bending in carboxylic acids) vanishes completely in the spectrum of the mixture. This evidence demonstrates the amide linkage formation between functional groups of the polymers. Additionally, the band at 1587 cm^{-1} in chitosan spectrum assigned to NH_2 deformation is shifted in the mixture to a significantly lower wavenumber (1529 cm^{-1}), which indicates the participation of chitosan primary amino groups in the reaction between polymers induced by the ultrasonication. The spectrum of the

polymer mixture extracted from the containers exhibits a new peak at 1493 cm^{-1} (amide II band) that reveals the formation of amide bonds. All these results confirm the chemical reaction between chitosan -NH_2 groups and -COOH of acetate or pyruvate groups in xanthan gum molecules caused by the ultrasound treatment.

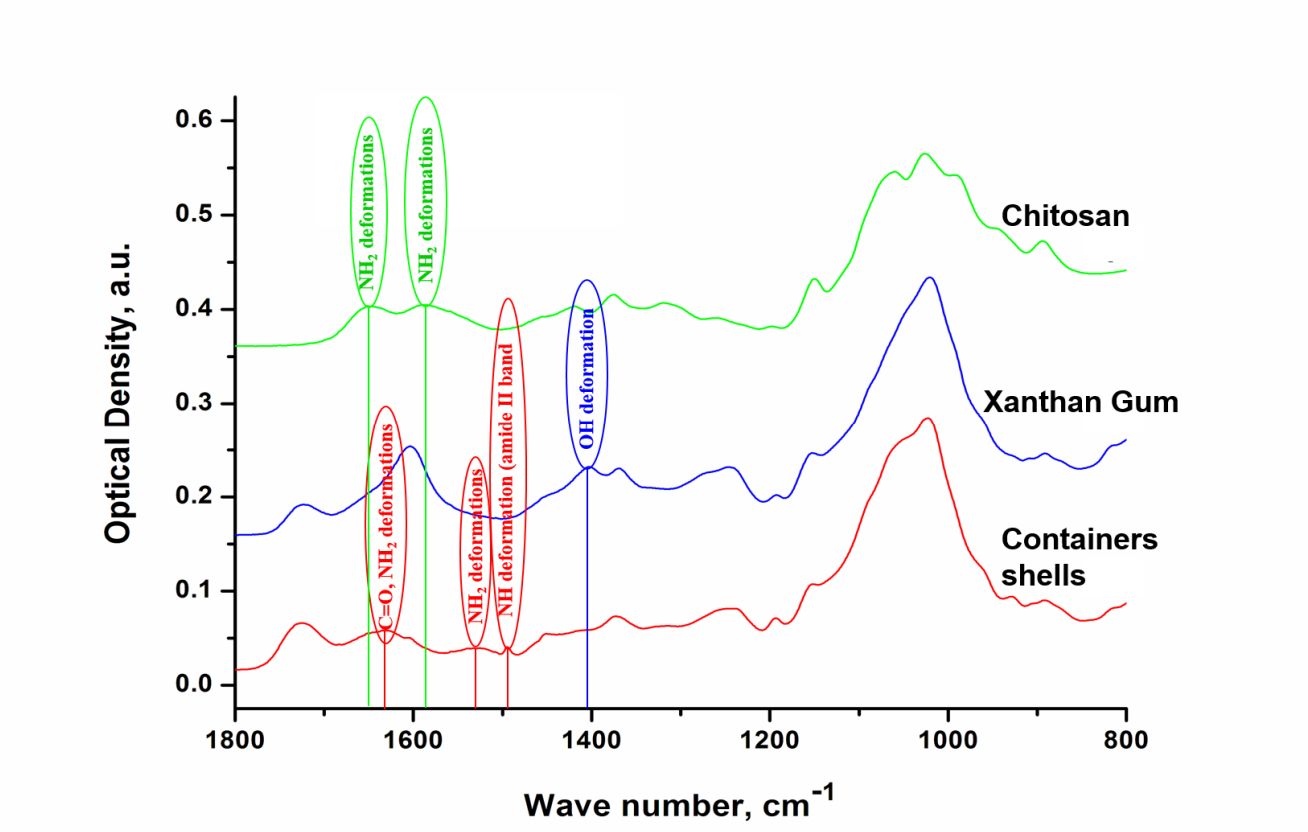

Figure 2. FTIR investigations of the pristine chitosan, xanthan gum and the polymer mixture treated with ultrasound (extracted from the microcontainers).

Changes in the FTIR spectrum of polysaccharide mixture registered after ultrasound-mediated microcontainer synthesis allow the assumption of the following mechanism of their formation. The acidic pH of the initial polymer solutions keeps xanthan gum in non-dissociated state and provides simultaneously a perfect solubility of chitosan. In the first step, the hydrogen bonds are formed between the polar groups (–COOH and –NH_2, -OH and –COOH) maintaining a primary

structure of the container shell. The second step consists of ultrasound induced formation of amide linkages which contribute to the final build-up of the permanent core-shell structure of microcontainer.

By varying an oil/water ratio (from 1:300 to 1:1.5, respectively), we easily obtained the containers in a wide size range (from 350±50 nm to 7500±500 nm), whose morphology and structure were investigated by cryo scanning electron microscopy (cryo-SEM) (Fig. 3) demonstrating well-separated containers with the narrow size distribution. The higher magnification image (Fig. 3C) of microcontainers with broken shells reveals their core/shell structure. The thin external polymer shell (Fig. 3C) surrounds inner container core. The estimated thickness of the shell is around 7-10 nm, which is however robust enough to keep the microcontainers stable during storage at 4ºC for at least 6 months. The container size changed from 1160±200 nm (PDI 0.417±0.08) to 1250±150 nm (PDI 0.504±0.1) over this period of storage.

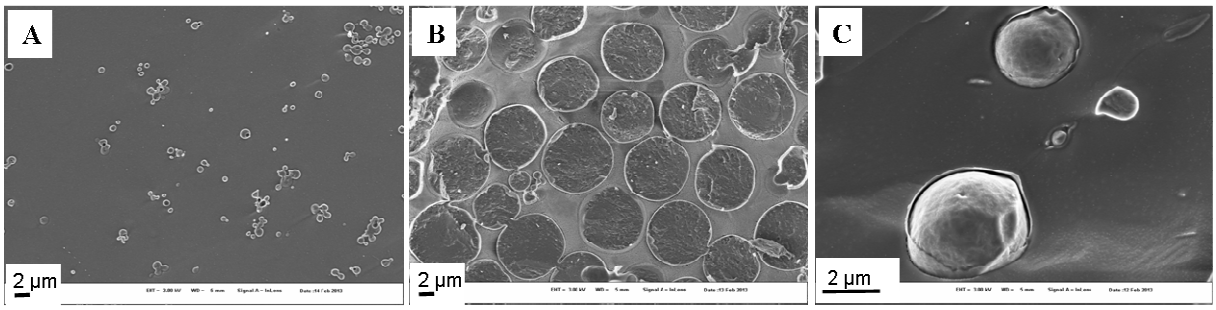

Figure 3. Cryo-SEM observations of the microcontainers with different size: A. 1160 nm (PDI 0.417), oil/water ratio 1/60; B. 7324 nm (PDI 0.146), oil/water ratio 1/1.5. C. Containers with broken shell.

The container size steadily decreases when the water phase/oil phase ratio increases. Figure 4 demonstrates dependence of the container size on the oil/water. This dependence can be

explained by changing an overall emulsion viscosity [29, 30]. Drops of emulsion placed in turbulent continuous phase (during ultrasonication) break upon the action of viscous or inertial stress acting on the drop surface. The regime of emulsification in turbulent flow can be changed from inertial to viscous one by the increase of the oil volume fraction, which leads to the change of the overall emulsion viscosity [30]. In the opposite case of the decreasing viscosity, the drop size in the emulsion is strongly reduced due to transition from the viscous to the inertial regime of the emulsification [29]. The soybean oil loaded microcontainers of 5.2 µm (PDI 0.389) size were used for further characterization.

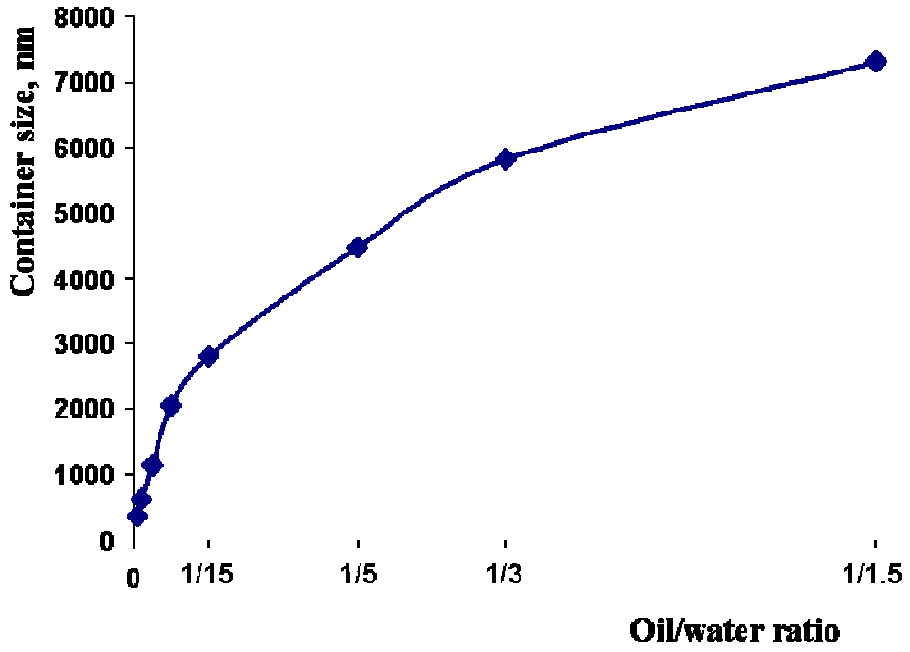

Figure 4. Dependence of the container size on the oil/water ratio. Each size value was averaged from five subsequent measurements each of 20 runs.

Polydispersities of all obtained emulsions were quite moderate (PDI $\leq$ 0.5) independently of oil/water ratio. This observation allows the assumption that not only mechanical forces but also some additional factors such as enthalpy and entropy changes during the emulsification can

contribute to the monodispersity of final systems. On the one hand, increase of the total area of the interface between oil and water phases in the emulsion should enhance the system enthalpy making the emulsion formation energetically unfavorable. On the other hand, the strong simultaneous increase of the entropy in the system can be considered as a significant benefit of the emulsification. The interplay of both these contributions (enthalpic and entropic) to the changes in the free Gibbs energy of the system lead to the most favorable and therefore stable state where the change in the free Gibbs energy of the system has a minimal positive value (because such systems as conventional emulsions are strictly speaking thermodynamically instable). This general consideration is consistent with the dependence of emulsion droplet size on the oil/water ratio: The lower is this ratio the smaller are the droplets and the higher is their total surface area but also the higher is their number and the corresponding increase of the entropy in the system. In the case of the high oil/water ratio increase of both enthalpic as well as entropic contributions upon emulsification is moderate because of larger droplets, i.e. of weaker increase of droplets surface area and disorder in the system, correspondingly. Consequently, the almost monodisperse emulsion but with larger droplets can be produced.

The images in Figure 5 show confocal laser scanning microscopy (CLSM) observation of the containers filled with solution of a fluorescent dye Nile Red in soybean oil, which surface was labeled by the deposition of PAH-FITC. The microphotographs demonstrate a presence of green fluorescence from the shell (adsorbed PAH-FITC, Fig. 5B) of the microcontainers with the red inner core (Fig. 5A). The Figure 5C confirms the core/shell morphology of obtained microcontainers as derived above on the basis of SEM. The measurements of Zeta-potential showed changes of the surface charge of microcontainers from -50 mV (initial containers) to +52 mV upon modification with cationic PAH-FITC. On the other hand, polymer adsorption has no

influence on the system stability. The microcontainers remain non-aggregated and well-dispersed also after their surface modification. Moreover, an interfacial attachment of negatively charged SiO_2 nanoparticles to the outer surface of PAH-coated container shell demonstrates further possibilities of container modification.

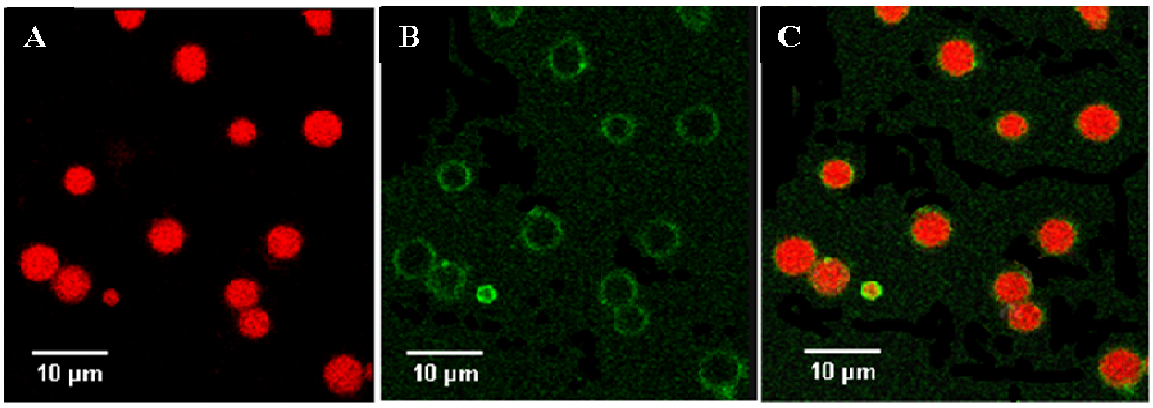

Figure 5. CLSM observation of the system modified by PAH-FITC (C), red emission from Nile Red (A), green - from PAH-FITC (B).

The main advantage of proposed approach for the container preparation is lack of use of environmentally harmful volatile organic compounds (VOC) or metal based catalysts, which are required for the most common container fabrication technique like spray-drying, polyaddition etc.

An excellent demonstration of the high practical relevance of developed containers is the successful encapsulation of the novel green biocide DCOIT for the further applications in aqueous antifouling coatings. DCOIT is a broad spectrum biocide with very good biodegradability and was recently recommended as environmentally friendly biocide for use in many different applications: wood preservation, plastics, sealants, marine antifouling and indoor coatings [31]. This biocide has low water solubility and therefore good leach resistance from the dried coatings contributing to its very sustained protection performance. The same peculiarity,

however, restricts the use of DCOIT to only solvent based coating formulations – it is almost impossible to distribute this substance homogeneously in an aqueous coating formulation leading finally to the violation of the coating integrity and to the subsequent loss of barrier properties of these coatings after curing. On the other hand, due to steadily raising environmental regulations limiting or even banning the use of VOC in many industrial fields, the development and application of water based coating formulations became more and more necessary. Successful implementation of highly hydrophobic DCOIT in aqueous coating formulations will therefore imply the development of new generation of very efficient and simultaneously eco-friendly antifouling paints.

Other advantage of the DCOIT loaded containers is the microbial triggering of their opening (Fig. 6A). Stimuli responsive regulation of the biocide release can be realized due to the bacterial decomposition of the container shell [32, 33]: The higher is the growth rate of the microorganisms population the stronger is the shell deterioration providing the active bacteriostatic feedback. The released biocide inhibits growth of the bacteria on the surface of coatings with the embedded containers, thereby imparting to them specific antimicrobial functionalities which can be on demand switched on.

Comparative agar diffusion tests for the evaluation of biocidic efficiency of the encapsulated DCOIT against three representative microorganisms: gram-positive bacteria *Bacillus subtilus* ATCC 6633, gram-negative bacteria *Escherichia coli* ATCC 25922 and mycelial fungus *Aspergillus niger* ATCC 16404 were performed (Fig. 6B) [34]. We examined two samples with encapsulated DCOIT: the initial microcontainers with biocide and the DCOIT containers coated with an additional layer of PAH. Two supplementary samples were prepared for control: a sample with containers without biocide and a sample with free distributed DCOIT. All samples

were placed on the surface of agar plate previously inoculated with the microorganisms to be tested. The plates were incubated at 37°C for 24 hours (in the case of bacteria) or at 28°C for 48 hours (in the case of fungus).

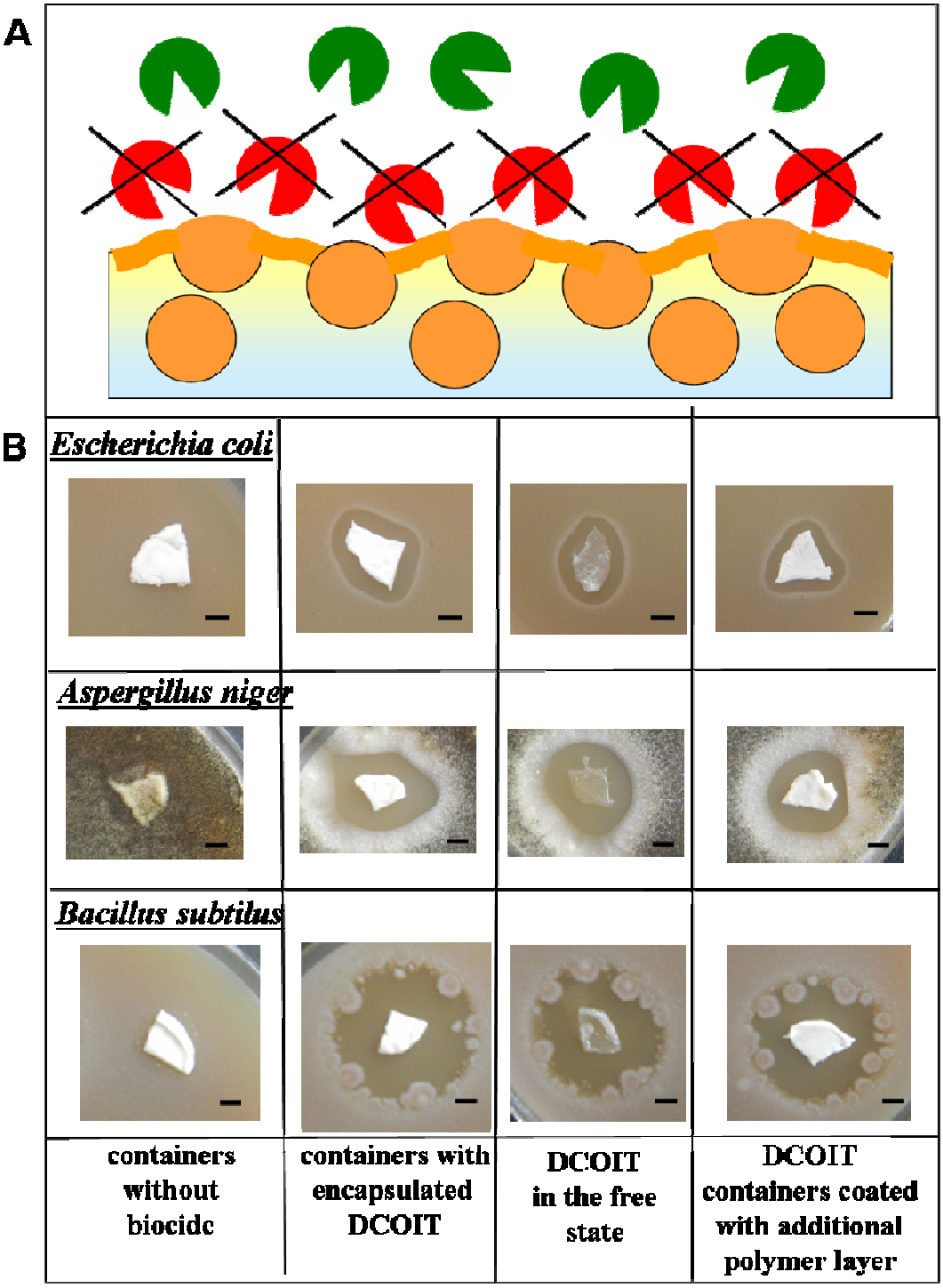

Figure 6. A. Scheme of microbial triggering of the container opening: bacterial decomposition of the container shell leads to release of encapsulated biocide followed by bacteria growth inhibition. B. Bacteriostatic activity of both encapsulated DCOIT and DCOIT in the free state against gram-positive bacteria Bacillus subtilus ATCC 6633, gram-negative bacteria Escherichia coli ATCC 25922 and mycelial fungus Aspergillus niger ATCC 16404 in Ca-alginate polymer film after 24 hours of incubation after 24 hours of incubation (scale bar is 5 mm).

Figure 6B demonstrates the presence of inhibition zones of bacterial growth (clear rings) around the sample with the biocide in freely dispersed state, around the sample with the encapsulated DCOIT and around the sample with the biocide containers modified with the PAH. The obtained results indicate a good diffusion of the biocide from the containers. We found a double zone of inhibition in the case of *Aspergillus niger* – the total zone of growth inhibition followed by the zone of sporulation inhibition. There was no inhibition zone around the sample without biocide (negative control) which evidences a non-toxicity of the container's material for the microorganisms.

The mode of DCOIT action is very fast and utilizes a two step mechanism involving rapid growth inhibition leading to a loss of viability [35]. In the case of the film with the embedded containers, the greatest inhibition effect was observed against *Bacillus subtilus* with a zone of inhibition of 26 mm followed by *Aspergillus niger* with a zone of inhibition of 21.5 mm and *Escherichia coli* with a zone of inhibition of 16 mm. We found slightly delayed DCOIT inhibition action in the case of the film with free distributed DCOIT (*Bacillus subtilus* – 24.2 mm, *Aspergillus niger* – 20 mm, *Escherichia coli* – 14.5 mm). The films with incorporated coated containers showed more sustained inhibition activity compare to previous samples: 23.2 mm of the inhibition zone against *Bacillus subtilus*, 17.7 mm – in the case of *Aspergillus niger*

and 14.6 mm against *Escherichia coli.* The results demonstrate that an additional coating with PAH decelerate the DCOIT diffusion from the film and thus could make its bacteriostatic activity essentially more sustained.

To compare a diffusion character of encapsulated DCOIT and DCOIT in the free state, we examined the activity of the samples against *Escherichia coli*. The encapsulated biocide showed an equal activity after 24 hours of incubation comparing to the same concentration of the freely dispersed DCOIT (10 µg/ml). The results after 48 hours of incubation demonstrate more sustained (around 30%) activity of DCOIT microcontainers indicating their prolonged performance in the coatings: 11.5 mm of inhibition zone for freely dispersed DCOIT versus 14 mm of inhibition zone for the encapsulated DCOIT (SI).

On the first glance, the biocide incorporated in the Ca-alginate matrix in free state should diffuse faster than encapsulated one. But in the reality, one has additionally to recognize (i) strong hydrophobicity of DCOIT and (ii) its significant instability against chemical degradation. The first factor leads to the aggregation of the DCOIT powder in the hydrophilic Ca -alginate matrix and, as a consequence, to the strong decrease of the total surface area of the DCOIT particles incorporated in the alginate. On the contrary, hydrophilicity of polysaccharide shells of DCOIT filled microcontainers provides essentially homogeneous distribution of these in the Ca-alginate matrix resulting in the much higher total surface area of all incorporated microcontainers filled with the same amount of DCOIT. Therefore, even in the case of lower diffusivity of the encapsulated DCOIT from the containers, the high total cross-section area of all containers participating in the release leads to the diffusion flux compatible or higher than one for the free incorporated biocide.

Moreover, the fast degradation of DCOIT in the free state contributes to the less sustained diffusion flux of the biocide especially in the long-term perspective. Thus, the inhibition zone for the microorganisms growth in case of the encapsulated (i.e. protected) DCOIT becomes after 48 hours exposition time broader than for the biocide incorporated in the free state. It is well-known from the literature that DCOIT rapidly degrades in marine and freshwater environments (half-life time <1 hour and <3 hours, respectively) and bioaccumulation of parent molecule is very low [36, 37]. Therefore, 48 hours of incubation could leads to the considerable biocide decomposition incorporated in the matrix in the free state while the encapsulation of the substance into the containers protect biocide from degradation and extend correspondingly the period of its bacteriostatic activity. These results are in agreement with [38], where authors demonstrate that degradation of DCOIT included in the paint particles leads to the increase of half-life until 10 days compare to less than 1 day for DCOIT in free form.

Additionally, postponed DCOIT bacteriostatic activity after 48 hours of incubation could be explained in view of mechanism of the biocide action. The mode of action of DCOIT is very fast. The biocide rapidly associated with microbial cells and inhibits a cellular activity within minutes [35].

To examine an influence of the polymer coating on the DCOIT-release level, we investigated the release rate of biocide for unmodified containers and containers coated with an additional polyelectrolyte (PAH). The release occurring is based on the diffusion of biocide from the containers confined in a dialysis tubing to an external aqueous phase. We observed the influence of the container modification on the rate of the DCOIT release. In the first hours, the polyelectrolyte coated containers showed the release of the biocide which was slower by a factor 2 comparing to unmodified ones (Fig. 7). Approximately 82% of DCOIT was released in 10

hours in the case of initial containers while modified containers showed only 70% of biocide released within the same period. The modification of the container surface impart prolonged release properties to the system presenting more sustained release of the encapsulated biocide.

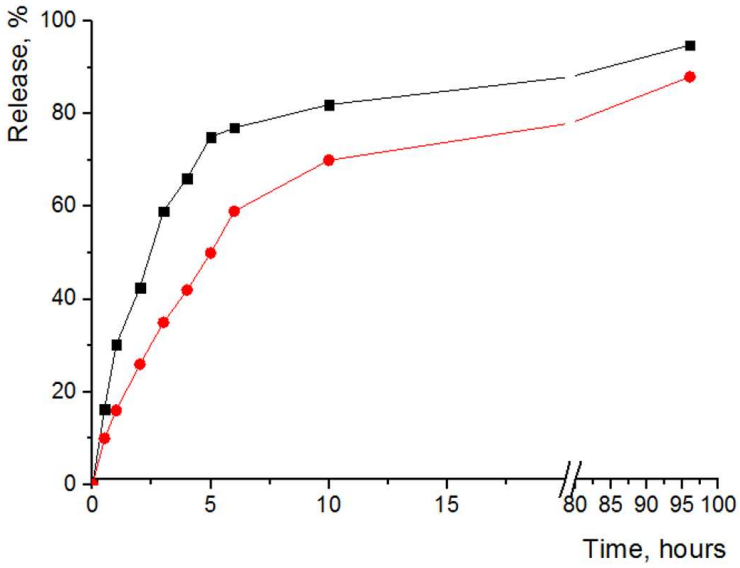

Figure 7. Release profile of DCOIT from the initial containers (■) and the containers modified with polymer layer (●).

DCOIT is a hydrophobic compound with very low water solubility. We performed the release experiment in sodium chloride solution (pH 7.5) maintaining the sink conditions for DCOIT. The more sustained release of DCOIT from the coated containers could be interpreted due to increase of the container shell hydrophilicity as the result of an additional polyelectrolyte layer (PAH) adsorption. Upon release from the containers, hydrophobic DCOIT has to penetrate through hydrophilic containers shells. Therefore, the increase of the diffusion path of DCOIT molecules within containers shells should lead to the slower release of the biocide. Moreover, hydrophobic-hydrophobic interactions between backbone chain of PAH and octyl chain of DCOIT can also contribute to the further slowing down of release.

These results are in a good agreement with previous observation where tests of bacteriostatic activity demonstrated a diminution of bacteria growth inhibition zone around the containers modified by the additional polymer layer compare to initial containers (Fig. 6B).

EXPERIMENTAL SECTION

Materials: Chitosan (20-300 cP), xanthan gum (from Xanthomonas campestris), polyallylamine hydrochloride (MW 70000), sodium alginate (medium viscosity), fluorescein isothiocyanate (FITC), soybean oil, hexane, cyclohexane, toluene were supplied from Sigma-Aldrich, Germany. 4,5-dichloro-2-n-octyl-4-isothiazoline-3-one (DCOIT) was purchased from Chemos GmbH, Germany. Miglyol 812 Neutral Oil (a mixture of medium chain caprylic/capric triglycerides, MCT) was provided by Sasol Germany GmbH, Witten, Germany, Batch: 080708. All materials were used without further purification.

Synthesize of container:

Equal volumes of chitosan and xanthan gum solutions (0.25w%, pH 2) were mixed, then layered with non-aqueous liquid and exposed to high-intensity ultrasound using a 7-mm diameter titanium sonotrode (56 $W \cdot cm^{-2}$, 20 kHz, 5 min) (Ultrasonic Processor UP400S, Hielscher Ultrasonics GmbH, Germany). The freshly prepared microcontainers were centrifuged (1.677 × g, 10 min), washed with water and then incorporated into a Ca-alginate film or modified with polyallylamine hydrochloride (PAH)) for fluorescent labelling and embedded into the polymer film. Sodium alginate was used here as a model polymer which easily forms the film by cross-linking with Ca^{2+}-ions. Namely, a mixture of 1 wt% sodium alginate solution and the containers was poured onto a cellulose filter (Millipore) saturated with 2 wt% $CaCl_2$ solution and covered by the same filter for 15 min. The cross-linked film was washed with physiological solution and kept in the fridge. In order to modify the container surface, they were incubated in PAH-FITC

solution (1 ml, 2 mg·ml^{-1}, 0.5M NaCl) under shaking (Vortex-genie 2, Scientific Industries, Inc., USA) at RT for 15 min. After the incubation, the containers were isolated by centrifugation (1.677 × g, 10 min) and washed three times with water to remove the polyelectrolyte excess.

Container characterization:

Fourier transform infrared (FTIR) measurements were performed with a Bruker Hyperion 2000 IR spectrometer at RT in KBr pellets. The pellets were fabricated from a mixture of polymer powder and potassium bromide using a manual pellet press (Specac, Orpington, U.K.) and mounted on a QuickLock base plate. Spectra between 400 to 4000 cm^{-1} were recorded with 2 cm^{-1} resolution in the transmission mode using a DTGS detector. For FTIR measurements, the microcontainers loaded with hexane were mechanically milled and to pounded with pestle. The polymers were dried in a desiccator for 3 hours, and the powder was investigated.

Confocal observations (CLSM) were carried out using a Leica TCS SP confocal scanning system (Leica, Germany) equipped with a 100×oil immersion objective (numerical aperture 1.4).

The morphology of the containers was studied using cryo-scanning electron microscopy. Each sample was frozen by plunging into nitrogen slush at atmospheric pressure. The samples were freeze-fractured at -150°C, etched for 60 s at -98°C, sputtered with platinum in the GATAN Alto 2500 Cryo preparation chamber, and then transferred into the Cryo-SEM.

The Z-potential and container size were measured by a Zeta Sizer Nano (Malvern Instruments, UK). Each Z-potential value was averaged from three subsequent measurement series each of 15 runs, and size value – from five subsequent measurements each of 20 runs.

Bacteriostatic activity test

Preparation of the containers: 5 ml of chitosan (0.25w%, pH 2) and 5 ml of xanthan gum (0.25w%, pH 2) were mixed, then layered with 500 µl of preheated up 45°C DCOIT and exposed

to high-intensity ultrasound using a 7-mm diameter titanium sonotrode (56 $W \cdot cm^{-2}$, 20 kHz, 5 min) (Ultrasonic Processor UP400S, Hielscher Ultrasonics GmbH, Germany). The freshly prepared microcontainers were centrifuged (1.677 × g, 10 min), washed with water and then incorporated into a Ca-alginate film or modified with PAH and embedded into the polymer film.

Preparation of polymer films: A mixture of 500 µl of 1 wt% sodium alginate solution and the containers was poured onto a cellulose filter (Millipore) saturated with 2 wt% $CaCl_2$ solution and covered by the same filter for 15 min. The cross-linked film was washed with physiological solution and kept in the fridge.

Following samples were prepared:

1. Ca-alginate film containing 50 µl of the containers loaded with soybean oil (negative control).

2. Ca-alginate film containing 50 µl of the containers loaded with DCOIT (42.5 µg of DCOIT).

3. Ca-alginate film containing 42.5 µg of DCOIT (positive control).

4. Ca-alginate film containing 50 µl of the DCOIT containers coated with PAH (42.5 µg of DCOIT).

Bacteriostatic activity of the samples was evaluated by comparative *agar diffusion tests* against three representative microorganisms: gram-positive bacteria *Bacillus subtilus* ATCC 6633, gram-negative bacteria *Escherichia coli* ATCC 25922 and mycelial fungus *Aspergillus niger* ATCC 16404. All samples were placed on the surface of agar plate previously inoculated with the microorganisms to be tested. The plates were incubated at 37°C for 24 hours (in the case of bacteria) or at 28°C for 48 hours (in the case of fungus). Antimicrobial activity was assessed as inhibition zones of bacterial growth around the samples.

Biocide release

DCOIT release profile was investigated using a dialysis method. Namely, 100 µl of encapsulated DCOIT were re-suspended in 5 ml of 0.5N NaCl solution and placed in a dialysis bag (Pur-A-Lyzer Mega 1000 Dialysis Kit Manual, PURG 10020, Sigma-Aldrich Labware, Germany). The dialysis kit was placed in sodium chloride release medium (50 ml). The study was performed in an incubator shaker at 300rpm at RT (BioShaker XP, Q.Instrument GmbH, Germany). At various time points, the release medium was completely replaced with fresh release medium and analyzed by UV-vis spectroscopy at 213 nm. The sink conditions were calculated based on DCOIT solubility, DCOIT amount contained in the containers, and total volume of release medium, and were maintained throughout the entire experimental time. Quantity of the released biocide was calculated and presented finally as a percentage (%) of its total entrapped amount.

CONCLUSIONS

In conclusion, we proposed a new type of the chitosan/xanthan gum microcontainers fabricated by the simple one-step ultrasound treatment. The used shell components – polysaccharides chitosan and xanthan gum are biocompatible, biodegradable and have lack of allergenicity. These containers can be on demand further modified with oppositely charged polyelectrolytes and/or particles. The subsequent successful embedding of containers with the encapsulated biocide DCOIT into the polymer coating showed the maintenance of the antibacterial activity of the biocide in the encapsulated state together with more sustained character of coating performance opening wide perspectives for the future applications of these containers in various types of functional coatings.

AUTHOR INFORMATION

Corresponding Author

*E-mail: borodina@crys.ras.ru

Author Contributions

The manuscript was written through contributions of all authors. All authors have given approval to the final version of the manuscript.

ACKNOWLEDGMENT

This work was supported by the RFBR 12-03-93939-ДЖИ8_а and NANOMAR "Nanocontainer-based active coatings for maritime applications" projects. Financial support from the European G8 project "Multiscale smart coatings with sustained anticorrosive action – smart coat" is gratefully acknowledged (D.G.). We would like to thank Olga A. Galatenko and Larisa P. Terekhova for the help with the microbiological experiments.

Supporting Information. FTIR spectra. Bacteriostatic activity test. This material is available free of charge via the Internet at http://pubs.acs.org.

REFERENCES

1. Shchukina E.M.; Shchukin D.G. LbL coated microcapsules for delivering lipid-based drugs. *Adv. Drug Delivery Rev.* **2011**, *63*, 837-846.

2. Grigoriev, D.O.; Haase, M.F.; Fandrich, N.; Latnikova, A.; Shchukin, D.G. Emulsion route in fabrication of micro and nanocontainers for biomimetic self-healing and self-protecting functional coatings. *Bioinspired, Biomimetic Nanobiomater*. **2012**, *1*(BBN2), 101-116.

3. Shchukina E.M.; Shchukin D.G. Layer-by-layer coated emulsion microparticles as storage and delivery tool. *Curr. Opin. Colloid Interface Sci*. **2012**, *17*, 281-289.

4. Li, G.L.; Möhwald, H.; Shchukin, D.G. Precipitation polymerization for fabrication of complex core-shell hybrid particles and hollow structures. *Chem. Soc. Rev*. **2013**, *42*, 3628-3646.

5. Grigoriev, D.O.; Miller, R. Mono- and multilayer covered drops as carriers. *Curr. Opin. Colloid Interface Sci*. **2009**, *14*, 48-59.

6. Agarwal, A; Lvov, Y; Sawant, R, Torchilin, V. Stable nanocolloids of poorly soluble drugs with high drug content prepared using the combination of sonication and LbL technology. *J. Controlled Release* **2008**, *128*, 255-260.

7. Leighton, T.G. *The Acoustic Bubble,* Academic Press Limited: London, 1994.

8. Deasy, P.B. *Microencapsulation and Related Drug Processes (Drug and Pharmaceutical Sciences)*, Marcel Dekker Inc: New York, 1984.

9. Donbrow, M. *Microcapsules and Nanocapsules in Medicine and Pharmacy*, CRC Press: Boca Raton, FL, 1991.

10. Webb, A.G.; Wong, M.; Kolbeck, K.J.; Magin, R.L.; Wilmes, L.J.; Suslick, K.S. Sonochemically Produced fluorocarbon Microspheres: A New Class Of Magnetic Resonance Imaging Agent. *Magn. Reson. Imaging* **1996**, *6*, 675–683.

11. Suslick, K.S.; Grinstaff, M.W. Protein Microencapsulation of Nonaqueous Liquids *J. Am. Chem. Soc*. **1990**, *112*, 7807-7809.

12. Wong, M.; Suslick, K.S. Sonochemically Produced Hemoglobin Microbubbles. *MRS Symp. Proc*. **1995**, *372*, 89-94.

13. Avivi, S.; Gedanken, A. S–S bonds are not required for the sonochemical formation of proteinaceous microspheres: the case of streptavidin. *Biochem. J.* **2002**, *366*, 705-707.

14. Dibbern, E.M.; Toublan, F. J.-J.; Suslick, K.S. Formation and characterization of polyglutamate core-shell microspheres. *J. Am. Chem. Soc.* **2006**, *128*, 6540-6541.

15. Tzhayik, O.; Cavaco-Paulo, A.; Gedanken, A. Fragrance release profile from sonochemically prepared protein microsphere containers. *Ultrason. Sonochem.* **2012**, *19*(4), 858-63.

16. Makino, K.; Mizorogi, T.; Ando, S.; Tsukamoto, T.; Ohshima, H. Sonochemically prepared bovine serum albumin microcapsules: factors affecting the size distribution and the microencapsulation yield. *Colloids Surf. B* **2001**, *22*(3), 251-255.

17. Teng, X.; Shchukin, D.G.; Möhwald, H. Encapsulation of water-immiscible solvents in polyglutamate/polyelectrolyte nanocontainers. *Adv. Funct. Mater.* **2007**, *17*, 1273-1278.

18. Avivi, S.; Gedanken, A. Are sonochemically prepared alpha-amylase protein microspheres biologically active? *Ultrason. Sonochem.* **2007**, *14*, 1-5.

19. Cavalieri, F.; Ashokkumar, M.; Grieser, F.; Caruso, F. Ultrasonic synthesis of stable, functional lysozyme microbubbles. *Langmuir* **2008**, *24*, 10078-10083.

20. Borodina, T.; Grigoriev, D.; Markvicheva, E.; Mohwald, H.; Shchukin, D. Vitamin E Microspheres Embedded Within a Biocompatible Film for Planar Delivery. *Adv. Eng. Mater*. **2011**, *13*(3), B123-B130.

21. Houdebine, L.-M. Production of pharmaceutical proteins by transgenic animals. *Comp. Immunol. Microbiol. Infect. Dis.* **2009**, *32*, 107-21.

22. Mihaela, M.E; Sardiu, E.; Cai, Y.; Jin, J; Swanson, S. K.; Conaway, R.C.; Conaway, J.W.; Florens, L.; Washburn, M.P. Probabilistic assembly of human protein interaction networks from label-free quantitative proteomics. *Proc. Natl. Acad. Sci. U.S.A.* **2007**, *105*(5), 1454-1459.

23. Şenel, S.; McClure, S.J. Potential applications of chitosan in veterinary medicine. *Adv. Drug Deliv. Rev.* **2004**, *56*, 1467-1480.

24. Dutta, P.K.; Dutta, J.; Tripathi, V.S. Chitin and chitosan: Chemistry, properties and applications. *J. Sci. Ind. Res.* **2004**, *63*, 20-31.

25. Katzbauer, B. Properties and Applications of Xanthan Gum. *Polym. Degrad. Stab*. **1998**, *59*, 81-84.

26. Sanderson, G.R. Application of Xanthan Gum. *Br. Polym. J.* **1981**, *13*, 71-77.

27. Jansson, P.E.; Kenne, L.; Lindberg, B. Structure of Extracellular Polysaccharide from Xanthomonas Campestris. *Carbohydr. Res.* **1975**, *45*, 275-82.

28. Aranaz, I.; Harris, R.; Heras, A. Chitosan amphiphilic derivatives: Chemistry and applications. *Curr.Org.Chem.* **2010**, *14*, 308-330.

29. Tcholakova, S.; Lesov, I.; Golemanov, K.; Denkov, N.D.; Judat, S.; Engel, R.; Danner, T. Efficient emulsification of viscous oils at high drop volume fraction. *Langmuir* **2011**, *27*, 14783-14796.

30. Vankova, N.S.; Denkov, N.D.; Ivanov, I.B.; Vulchev, V.; Danner, T. Emulsification in turbulent flow 1. Mean and maximum drop diameters in inertial and viscous regimes. *J. Colloid Interface Sci*. **2007**, *312*, 363-380.

31. Document II-A: Study Summaries–Dossier for Active Substance 4,5-Dichloro-2-octyl-4-isothiazolin-3-one (DCOIT), Product type 10, *Masonry preservatives, RMS: Norway, Rohm and Haas Company* 2010, 1-18.

32. Gooday, G.W. Physiology of microbial degradation of chitin and chitosan. *Biodegradation* **1990**, *1*(2), 177-190.

33. Cadmus, M.C.; Slodki, M.E. *Bacterial degradation of xanthan gum.* Industrial Polysaccharides. Genetic Engineering, Structure/Property Relations and Applications (Progress in Biotechnology 3); Elsevier Science Publishers: Amsterdam, Oxford, New York, Tokyo, 1987.

34. National committee for clinical laboratory standards. Reference method for broth dilution antifungal susceptibility testing of conidium-forming filamentous fungi: Approved standard M38-A. NCCLS. Wayne, PA, USA, 2002.

35. Williams, T.M. The mechanism of action of isothiazolone biocide. PowerPlant Chem. **2007**, 9(1), 14-22.

36. Jacobson, A.H.; Willingham, G.L. Sea-Nine antifoulant: an environmentally acceptable alternative to organotin antifoulants. *Sci. Total Environ*. **2000**, *258*(1-2), 103-10.

37. Thomas, K.V.; McHugh, M.; Waldock, M. Antifouling paint booster biocides in UK coastal waters: Inputs, occurrence and environmental fate. *Sci. Total Environ*. **2002**, *293*(1-3), 117-27.

38. K.V. Thomas, M. McHugh, M. Hilton, M. Waldock. Increased persistence of antifouling paint biocides when associated with paint particles. *Environ. Pollut*. **2003**, *123*(1), 153-61.

For Table of Contents Only